



HAL
open science

NMF HYPERSPECTRAL UNMIXING OF THE SEA BOTTOM: INFLUENCE OF THE ADJACENCY EFFECTS, MODEL AND METHOD

M Guillaume, L Juste, X Lenot, Y Deville, B Lafrance, M Chami, S Jay, A
Minghelli, X Briottet, V Serfaty

► **To cite this version:**

M Guillaume, L Juste, X Lenot, Y Deville, B Lafrance, et al.. NMF HYPERSPECTRAL UNMIXING OF THE SEA BOTTOM: INFLUENCE OF THE ADJACENCY EFFECTS, MODEL AND METHOD. 9th Workshop on Hyperspectral Image and Signal Processing: Evolution in Remote Sensing (WHISPERS 2018), Sep 2018, Amsterdam (NETHERLANDS), Netherlands. hal-04719553

HAL Id: hal-04719553

<https://hal.science/hal-04719553v1>

Submitted on 3 Oct 2024

HAL is a multi-disciplinary open access archive for the deposit and dissemination of scientific research documents, whether they are published or not. The documents may come from teaching and research institutions in France or abroad, or from public or private research centers.

L'archive ouverte pluridisciplinaire **HAL**, est destinée au dépôt et à la diffusion de documents scientifiques de niveau recherche, publiés ou non, émanant des établissements d'enseignement et de recherche français ou étrangers, des laboratoires publics ou privés.

NMF HYPERSPECTRAL UNMIXING OF THE SEA BOTTOM: INFLUENCE OF THE ADJACENCY EFFECTS, MODEL AND METHOD

M. Guillaume¹, L. Juste¹, X. Lenot², Y. Deville³, B. Lafrance², M. Chami⁴, S. Jay¹, A. Minghelli⁵, X. Briottet⁶, V. Serfaty⁷

1: Aix Marseille Univ, CNRS, Centrale Marseille, Institut Fresnel, F-13013 Marseille, France

2: CS Systemes d'Information, 31506 Toulouse Cedex 05, France

3: IRAP, Observatoire Midi-Pyrénées, Université de Toulouse, UPS-CNRS-OMP, 31400 Toulouse, France

4: Sorbonne Universités, UPMC Univ Paris 06, INSU-CNRS, LATMOS, 06230 Villefranche sur Mer, France;

5: Université de Toulon, CNRS, SeaTech, LIS laboratory, UMR 7296, 83041 Toulon, France

6: ONERA/DOTA, BP74025 - 2 avenue Edouard Belin, FR-31055 TOULOUSE CEDEX 4

7: DGA/DS/MRIS, 75509 Paris Cedex 15, France

ABSTRACT

Sea bottom unmixing is a challenging task for the analysis of coastal zones. Actually the upward photons are attenuated and diffused by the water column layer, giving low signal to noise hyperspectral data. A classical approach is to perform inversion of the water column using semi-analytical parametric models and estimation process, and obtain the water column constituents (chlorophyll, suspended matter, dissolved organic matter and bathymetry), and the coefficients of pure materials reflectance spectra (endmembers), given in spectral libraries, for each pixel. We consider here the case of unknown endmembers, and we suppose that the water column components have been obtained by a classical inversion method or in-situ measurements. For each observed pixel the upward luminance is analysed and decomposed into three terms, respectively issued after interaction with the target bottom pixel, its neighbours, and the water column. We show that in some conditions the adjacent pixels effect is not negligible, due to the diffusion in the water column, and we develop in accordance a new mixing model for the sea bottom. We propose a non-negative matrix factorisation based unmixing method to solve the problem, and present results for hyperspectral data simulations.

1. INTRODUCTION

For the last decades, hyperspectral airborne remote-sensing has been widely used for mapping of water composition and bathymetry. In coastal environments, hyperspectral remote sensing methods that allow the simultaneous retrieval of bathymetry, water quality and benthic cover are usually based on a radiative transfer model that describes how light propagates in water. Semi-analytic parametric models have

been developed to describe the relation between the bottom reflectance and remote-sensing reflectance by taking into account water attenuation [1], [2], and also numerical models such as Hydrolight [3]. These models usually consider that four parameters affect the water-leaving radiance: depth and concentrations of optically active constituents, i.e., chlorophyll (*Chl*), colored dissolved organic matter (*Cdom*) and suspended non-algal particles (*SM*) [4]. The inverse problem is generally solved using either look-up tables or iterative least square optimization [4], or maximum Likelihood (ML) [5], [6], with the help of a known bottom spectral library. Unmixing consists in estimating both abundances fractions and endmember spectra in each observed pixel. Actually, due to natural variability, existing fixed spectral libraries do not always really represent the materials for a given observation, generally supposed to be a linear combination of the end-member spectra with abundance coefficients. Interestingly, The non-negative matrix factorization (NMF) method has shown to be able to adapt to various mixing models [7]. In the case of seabed analysis, the water column influence must be included in the model. In [8] we have used Lee's radiative transfer model and proposed to combine ML estimation and NMF unmixing to obtain simultaneously the water parameters, the endmembers and the relative abundances. In this study, we propose to refine the radiative transfer model and develop an adapted NMF based unmixing method, making the hypothesis that the water column parameters can be previously obtained, either with in-situ measurements and bathymetric maps, or by the mean of a classical inversion method that would not require the precise knowledge of the bottom, or else by inversion with a fixed spectral library. Then the results of the inversion can be used to initialize the spectra and the abundance coefficients for the unmixing. In order to develop a refined radiative transfer model, we first consider analytically the various sources of upward light issued from the water column, and in a second step make use of the soft-

Thanks to French Defense Agency for funding within the ANR/astrid HypFoM 15-ASTR-0019

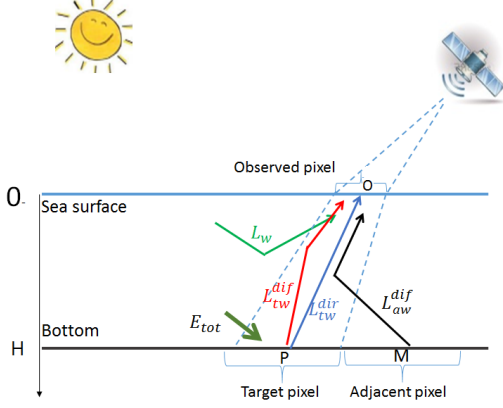


Fig. 1. Upward subsurface radiance

ware OSOAA [9] to simulate those many contributions to the total upward luminance. We note that in some situations the contribution of the bottom pixels adjacent to the target one cannot be neglected in the total leaving radiance, so we keep the corresponding terms in the radiative transfer model. In the section 3 we develop the corresponding mixing model, and we solve this problem with an NMF procedure. Last, we present the unmixing results for realistic simulated data.

2. RADIATIVE TRANSFER MODEL

In this section, we analyse the radiative transfer model within the oceanic layer, from the bottom to subsurface level, and we simulate the different sources of upward light at the underwater surface.

2.1. Analytical expression of the subsurface upward radiance

If we consider only the first order terms, the upward subsurface radiance when observing a subsurface pixel O can be decomposed as presented in figure 1, with bold terms corresponding to spectral vectors:

\mathbf{E}_{tot} : total downward luminance at the bottom level.

\mathbf{L}_{tot} : total subsurface upward radiance

\mathbf{L}_{tw}^{dir} : subsurface direct upward radiance after interaction with the target

\mathbf{L}_{tw}^{dif} : subsurface diffuse upward radiance after interaction with the target

\mathbf{L}_{aw}^{dif} : subsurface diffuse upward radiance after interaction with the pixels adjacent to the target

\mathbf{L}_w : subsurface diffuse upward radiance from the water column, without interaction with the bottom

It can be seen in figure 1 that when observing a subsurface pixel O , the environment of the target pixel P of the bottom contribute to the observed subsurface radiance, due to the diffusion of light inside the water column. Then the total contributing bottom reflectance is not only the target pixel,

but also its neighbours. The observed sub-surface radiance at depth 0_- , corresponding to the target bottom pixel P , can be expressed by the sum of three main terms (figure 1):

$$\mathbf{L}_{tot}(0_-) = \mathbf{L}_{tw}^{dir}(0_-) + \mathbf{L}_{env}^{dif}(0_-) + \mathbf{L}_w(0_-) \quad (1)$$

and $\mathbf{L}_{env}^{dif}(0_-) = \mathbf{L}_{tw}^{dif}(0_-) + \mathbf{L}_{aw}^{dif}(0_-)$.

In the following, we omit the depth 0_- for the subsurface luminance terms.

In the next section we focus on the equivalent environment reflectance of the bottom, including the target pixel and its neighbours.

2.2. Environment reflectance

We consider the equivalent bottom environment reflectance, including the target pixel and the adjacent ones, that contribute to the upward diffuse radiance for one pixel observed. It is defined as the spectral vector ρ_{env} :

$$\rho_{env}(\lambda, P) = \int \int_{M \in \mathcal{V}(P)} \gamma_{env}(\lambda, d(P, M)) \rho(\lambda, M) dS \quad (2)$$

M is a pixel in the neighbor $\mathcal{V}(P)$ of P , $\rho(\lambda, M)$ the bottom reflectance at pixel M , dS is the elementary surface around M , γ_{env} the environment function for the upward radiance, and $d(P, M) = R$ is the distance between P and M .

Formally, the environment function is dependent on the wavelength, but we have verified with simulations that it varies very slowly with it, so we shall consider this function as a scalar in the equation 2. It is given by $\gamma_{env}(P, M) = \frac{1}{S} \frac{dG(R)}{dR}$, with S the environment surface, and $G(R)$ the contribution of a target pixel of radius R (pixel size) to the environment $\mathcal{V}(P)$ for the total diffuse radiance at subsurface level. For the upward diffuse radiance, the diffusion is anisotropic from the bottom to the sea surface, so the environment function is not symmetric. In this case, the expression of $G(R)$ can be found in [10], and depends on the optical thickness of the water layer and the phase function. Then it varies with the depth H , the water quality, given by $[Chl, Cdom, SM]$, and the wavelength. $G(R)$ has been calculated by means of OSOAA simulations, for many values of depth, wavelength, water quality and target pixel size R . Some values of the environment function are plotted in figure 2, for a standard quality water $[Chl = 1 \text{ mg}/\text{m}^3, Cdom = 0.2 \text{ m}^{-1}, SM = 3 \text{ mg}/\text{L}]$, as a function of R (the results were the same for all wavelengths between 400 nm and 700 nm). We note that the contribution of a 0.20 m target pixel in the diffuse light, given by $G(R)$, is approximately 75% for 1 m depth, while it is only 40% at 5 m . Consequently, the pixels neighbour to the target one cannot be neglected in high resolution images.

The total environment reflectance at pixel P is then, separating target and adjacent pixels contributions:

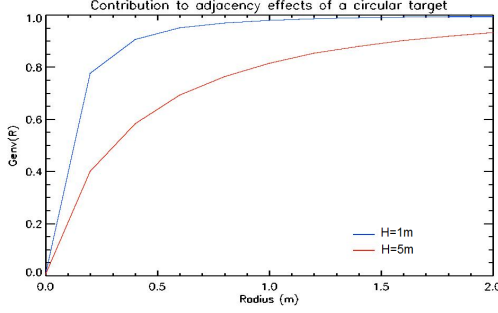


Fig. 2. Environment function $G(R)$ for many pixel sizes, two depths, and standard water

$$\begin{aligned} \rho_{env}(P) &= \rho_t(P) \int \int_{M=P} \gamma_{env}(R) dS + \\ &\quad \rho_a(P) \int \int_{M \neq P} \gamma_{env}(R) dS \\ \rho_{env} &= \delta \times \rho_t + (1 - \delta) \times \rho_a \end{aligned} \quad (3)$$

$\rho_t(P)$ is the target reflectance, $\rho_a(P)$ the equivalent reflectance of the pixels in the neighbour of the target. The radiative transfer equation becomes:

$$\begin{aligned} \mathbf{L}_{tot}(0_-) &= \mathbf{L}_w(0_-) + \frac{\mathbf{E}_{tot}(P)}{\pi} \odot \mathbf{T}_{dir}(0_-) \odot \rho_t \\ &+ \frac{\mathbf{E}_{tot}(P)}{\pi} \odot \mathbf{T}_{dif}(0_-) \odot [\delta \times \rho_t + (1 - \delta) \times \rho_a] \end{aligned} \quad (4)$$

The environment parameter δ (resp. $1 - \delta$) gives the proportion of diffuse light rising to the surface after interaction with the target (resp. adjacent pixels). \odot is the Hadamard (pointwise) product, \mathbf{T}_{dir} is the direct upward transmission vector, \mathbf{T}_{dif} the diffuse upward transmission vector and $\mathbf{E}_{tot}(P)$ the total illumination at the bottom pixel P .

In order to obtain a usefull expression for unmixing, we now introduce the mixing model into the radiative transfer equation.

2.3. Decomposition of the bottom reflectances

2.3.1. Target pixel

The target pixel is decomposed as a linear combination of J endmembers \mathbf{s}_j : $\rho_t = \sum_j \mathbf{s}_j a_{j,t}$, with $a_{j,t}$ being the abundance fraction of the 'pure' material of reflectance \mathbf{s}_j in the target pixel t .

2.3.2. Environment reflectance

Let call N the number of adjacent neighbours considered in the scene. $\rho_a = \frac{1}{N} \sum_{n=1}^N \rho_n$, ρ_n being the reflectance

at pixel n , in the neighbour of the target pixel, and ρ_n can also be decomposed as a linear endmembers mixture $\rho_n = \sum_{j=1}^J a_{j,n} \mathbf{s}_j$, with $a_{j,n}$ the abundance fraction of the j^{th} endmember in the pixel ρ_n .

When observing the target pixel O_i at subsurface level, the diffuse light comes both from the target bottom pixel P_i and from the adjacent pixels. The parameter δ is dependent on the pixel, because the depth and the water quality can vary in the scene. The equivalent reflectance spectrum corresponding to this observation is defined as:

$$\begin{aligned} \rho_{env,i} &= \delta_i \rho_{t,i} + (1 - \delta_i) \rho_{a,i} \\ &= \delta_i \sum_{j=1}^J a_{j,i} \mathbf{s}_j + (1 - \delta_i) \frac{1}{N} \sum_{n=1; n \neq i}^N \sum_{j=1}^J a_{j,n} \mathbf{s}_j \\ &= \sum_{j=1}^J \left[\sum_{n=1}^N p_{n,i} a_{j,n} \right] \mathbf{s}_j \end{aligned} \quad (5)$$

with $p_{n,i} = \frac{1 - \delta_i}{N}$ if $n \in \mathcal{V}(i)$, $n \neq i$, $p_{n,i} = \delta_i$ if $n = i$, and else $p_{n,i} = 0$. This can be written with a vector/matrix product: $\rho_{env}(i) = \mathbf{S} \tilde{\mathbf{a}}_i$, with \mathbf{S} the matrix containing all the endmembers arranged in columns, and $\tilde{\mathbf{a}}_i$ a vector whose the j^{th} element is $\tilde{a}_{j,i} = \sum_{n=1}^N a_{j,n} p_{n,i}$.

Finally, each component of $\tilde{\mathbf{a}}_i = \mathbf{A} \mathbf{p}_i$ gives an 'equivalent abundance' with the weighted sum of the proportions of the endmembers in the whole neighbour of the target pixel i , and $\rho_{env}(i) = \mathbf{S} \mathbf{A} \mathbf{p}_i$

3. UNDERWATER MIXING PROBLEM

3.1. Mixing model

We obtain the mixing model from the radiative transfer equation, divided by the downward illumination at surface level, $\mathbf{E}(0_-)$ in order to obtain reflectances ($/$ is the pointwise division).

$$\begin{aligned} (\mathbf{L}_{tot} - \mathbf{L}_w) ./ \mathbf{E}(0_-) &= \\ (\mathbf{E}(P) ./ \pi \mathbf{E}(0_-)) \odot [\mathbf{T}_{dir} \odot \rho_t + \mathbf{T}_{dif} \odot \rho_{env}] \end{aligned} \quad (6)$$

For each target pixel i we have: $\tilde{\mathbf{r}}_i = \mathbf{k}_1 \odot (\mathbf{S} \mathbf{a}_i) + \mathbf{k}_2 \odot (\mathbf{S} \mathbf{A} \mathbf{p}_i)$, with $\tilde{\mathbf{r}}_i = (\mathbf{L}_{tot} - \mathbf{L}_w) ./ \mathbf{E}(0_-)$, $\mathbf{k}_1 = (\mathbf{E}(P) ./ \pi \mathbf{E}(0_-)) \odot \mathbf{T}_{dir}$ and $\mathbf{k}_2 = (\mathbf{E}(P) ./ \pi \mathbf{E}(0_-)) \odot \mathbf{T}_{dif}$. For the whole scene, the mixing model is then:

$$\tilde{\mathbf{R}} = \mathbf{K}_1 \odot (\mathbf{S} \mathbf{A}) + \mathbf{K}_2 \odot (\mathbf{S} \mathbf{A} \mathbf{P}) \quad (7)$$

The $L \times I$ matrices $\tilde{\mathbf{R}}$, \mathbf{K}_1 , \mathbf{K}_2 are constructed with all the spectral vectors arranged in columns, the abundance matrix \mathbf{A} is $J \times I$ and \mathbf{P} is $I \times I$.

This model is a generalisation of the linear mixing model to the case of diffused photons, being the cause of adjacency effects described by the additive term ($\mathbf{K}_2 \odot \mathbf{S} \mathbf{A} \mathbf{P}$).

We propose a generalisation of the non negative matrix procedure to solve this mixing problem.

3.2. Unmixing method

The unmixing problem is the estimation of both matrices \mathbf{A} and \mathbf{S} . Actually In this work we consider the case where only the bottom is unknown, the water column illumination, transmission, diffusion vectors being all known. The matrix \mathbf{P} is preliminary calculated for a given neighbour of the target pixel, depending on the pixel size, and is fixed in the optimisation process.

In order to solve the problem, we minimize a cost function that is the Frobenius norm between the observed subsurface reflectance (corrected by the water subsurface reflectance), and the estimated one:

$$RQE = \|\tilde{\mathbf{R}}_{obs} - \tilde{\mathbf{R}}\|_{Fro}^2$$

Where $\tilde{\mathbf{R}}_{obs}$ is the observed reflectance, corrected from the water radiance. We solve the optimisation with a non negative matrix factorisation scheme. We use an alternate projected gradient. The cost function gradients up to \mathbf{A} and \mathbf{S} are:

$$\begin{aligned} \nabla RQE_S(\mathbf{S}, \mathbf{A}) &= \\ &\left[\mathbf{K}_1 \odot \left(\tilde{\mathbf{R}}_{obs} - \mathbf{K}_1 \odot (\mathbf{S}\mathbf{A}) - \mathbf{K}_2 \odot (\mathbf{S}\mathbf{A}\mathbf{P}) \right) \right] \mathbf{A}^t \\ + \mathbf{K}_2 \odot \left[\left(\tilde{\mathbf{R}}_{obs} - \mathbf{K}_1 \odot (\mathbf{S}\mathbf{A}) - \mathbf{K}_2 \odot (\mathbf{S}\mathbf{A}\mathbf{P}) \right) \right] (\mathbf{A}\mathbf{P})^t \\ \nabla RQE_A(\mathbf{S}, \mathbf{A}) &= \\ &\mathbf{S}^t \left[\mathbf{K}_1 \odot \left(\tilde{\mathbf{R}}_{obs} - \mathbf{K}_1 \odot (\mathbf{S}\mathbf{A}) - \mathbf{K}_2 \odot (\mathbf{S}\mathbf{A}\mathbf{P}) \right) \right] \\ + \mathbf{S}^t \left[\mathbf{K}_2 \odot \left(\tilde{\mathbf{R}}_{obs} - \mathbf{K}_1 \odot (\mathbf{S}\mathbf{A}) - \mathbf{K}_2 \odot (\mathbf{S}\mathbf{A}\mathbf{P}) \right) \right] \mathbf{P}^t \end{aligned}$$

The unmixing algorithm is then

Algorithm 1 NMF Underwater Unmixing algorithm

Initialization : estimation of $\mathbf{K}_1, \mathbf{K}_2, \mathbf{A}_{init}, \mathbf{S}_{init}$
while $\epsilon > th$ **do**
 $\{\mathbf{A}^{(n+1)}\} \leftarrow \{[\mathbf{A}^{(n)} - \alpha_A \nabla RQE_A(\mathbf{S}^n, \mathbf{A}^n)]_0^1\}$
 $\{\mathbf{S}^{(n+1)}\} \leftarrow \{[\mathbf{S}^{(n)} - \alpha_S \nabla RQE_S(\mathbf{S}^n, \mathbf{A}^n) + reg_S]_0^1\}$
 $\tilde{\mathbf{R}}^{(n+1)} = \mathbf{K}_1 \odot (\mathbf{S}^{(n+1)}\mathbf{A}^{(n+1)}) + \mathbf{K}_2 \odot (\mathbf{S}^{(n+1)}\mathbf{A}^{(n+1)}\mathbf{P})$
 $\epsilon = \max_p (|\tilde{\mathbf{r}}^{(n+1)} - \tilde{\mathbf{r}}^{(n)}| / \tilde{\mathbf{r}}^{(n)})$
 $n = n + 1$
end while

α_A and α_S are the gradient steps, calculated with an Armijo-Lin method. We also use regularization for the endmembers, given by reg_S , as defined in [11], to minimise endmembers dispersion. The results are assessed with simulated images. In future work, we shall also make the water column characteristics be unknown, but here we restrict the problem to the estimation of the bottom.

3.3. Simulations

We develop simulations in order to assess the proposed method. Data are simulated according to the model, and

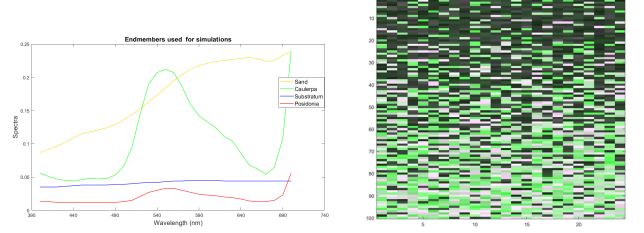


Fig. 3. Endmembers spectra and simulated bottom in reconstructed colors

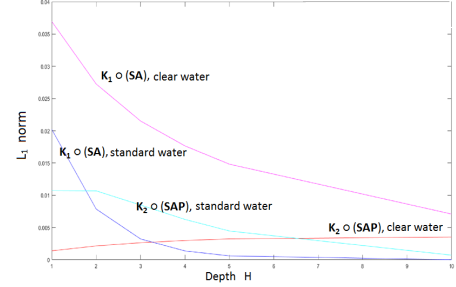


Fig. 4. L_1 norm of the different terms in the mixing model

the unmixing is performed with the proposed NMF. The results are evaluated with quadratic error on the spectra, abundances and reconstructed subsurface image, and spectral angle distance for the endmembers.

3.3.1. Simulated data

The bottom is generated with a linear mixing model, using four endmember spectra representative of the benthic species, in (figure 3), that have been obtained through a data campaign, made in the area of Porquerolles Island, South France, in September 2015. There are representative of two algae, the Caulerpa Taxifolia, and the Posidonia, clear sand and a dark substratum. In order to reduce the time calculation done by OSOAA for each pixel, we have sub-sampled the spectra and only 31 wavelengths are kept between 400 nm and 700 nm, to account for the water attenuation out of this spectral band. The abundances are randomly generated with a maximum abundance of 85% for each endmember, though we have enforced the mixing between the two clear spectra or the two dark spectra in order to have a good contrast, and the relative quantities of light or dark mixed pixels vary in five zones of the image (figure 3).

The values of \mathbf{K}_1 and \mathbf{K}_2 determine the relative importance of the diffused light and direct light. We show the L_1 norms of the direct and the diffuse terms, for clear and standard water and many depths in figure 4. We note that generally the direct term dominates the diffuse term, so the influence of the adjacency effect, only present in the diffuse term, will not be noticeable. However in high depth, the dif-

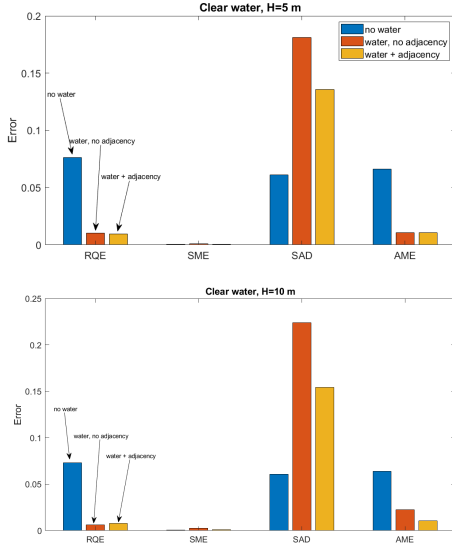


Fig. 5. Reconstruction errors, errors on spectra and abundances for the three unmixing

fusion term is comparable to the direct term, so in this case the new model should be performing. We generate the underwater data according to equation 7, with $H = \{5 m, 10 m\}$ and clear water. Some white noise is added to the subsurface image, in order to attain a SNR of 40dB.

3.3.2. Results

We initialize the unmixing either with VCA performed on the bottom without water added, or with endmembers modified with a correlated Gaussian law. The abundances are initialized with FCLS applied on the bottom. We present results for a pixel radius $R = 0.5 m$, at $H = 10 m$ and $H = 5 m$, averaged on 10 realizations and the two different initializations, and calculate the mean square error on reconstructed bottom (RQE), on endmembers (SME) and abundances (AME), and the spectral mean error on endmembers (SAD). We compare the results when using the model of equation 7 for the unmixing, and when performing the unmixing with no adjacency effect modeled (no adjacency model : $\mathbf{R} = \mathbf{K}_1 \odot (\mathbf{S} \mathbf{A}) + \mathbf{K}_2 \odot (\mathbf{S} \mathbf{A})$), then neglecting the adjacency pixels effects in the diffusion term. This allows to assess the relevance of the complete model. We also compare with the unmixing of the bottom without any water column, which obviously gives the best performances.

Figure 5 shows that the complete model is performing better than the model with no adjacency effects, for $H = 10 m$ and $H = 5 m$, and clear water. In figure 6 we present in detail the spectral mean error for the three unmixing at $H = 10m$, with the error bars showing some variability.

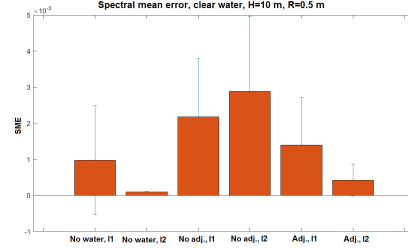


Fig. 6. Spectral mean error, three unmixing, two initializations

4. CONCLUSION

In this work we have developed a new unmixing scheme, adapted to the sea bottom analysis. To this end we have proposed a new mixing model that takes into account the diffusion effects inside the water column, leading to bottom adjacency effects. We make use of the software OSOAA to simulate precisely the water column effects onto the upwelling photons, and we evaluate the results with realistic simulations. The results mainly depends on the pixel size, the depth and the water quality. We show that for pixels of radius $R = 0.5 m$ the model is able to improve the results for depths $\geq 5 m$ in clear water. Then we conclude that for high resolution sensors the bottom estimation is improved by taking into account the proposed model, that account for the bottom adjacency effects. In future work we will present more deeply the analysis of the model, and apply it to many different simulated cases, as well as to unmixing of real images. Moreover we have here supposed known the water characteristics, in future works we will also suppose those unknown and develop the corresponding method.

5. REFERENCES

- [1] Z. Lee, K. Carder, C. Mobley, R. Steward, and J. Patch, *App. Optics*, vol. 37, pp. 6329–6338, 1998.
- [2] S. Maritorena, A. Morel, and B. Gentili, *Limnology and Oceanography*, vol. 39, pp. 1689–1703, 1994.
- [3] C. Mobley, “Light and water: Radiative transfer in natural waters,” *Academic Press*, 1994.
- [4] A. G.Dekker, S. R.Phinn, J.Anstee, P.Bissett, V. E.Brande, and B.Casey, *Limn. and Oceano.: Methods*, vol. 9, p. 396, 2011.
- [5] S. Jay and M. Guillaume, *Rem. Sens. of Env.*, vol. 147, p. 121.
- [6] S. Jay, M. Guillaume, A. Minghelli, Y. Deville, M. Chami, B. Lafrance, and V. Serfaty, *Rem. Sen. of Env.*, vol. 200, pp. 352–367, 2017.
- [7] I. Meganen, Y. Deville, S. Hosseini, P. Deliot, and X. Briottet, *IEEE TGRS*, vol. 62, pp. 1822–1833, 2014.
- [8] M. Guillaume, Y. Michels, and S. Jay, in *WHISPERS*, Tokyo, Japan, June 2015.
- [9] M. Chami, B. Lafrance, B.Fougny, J. Chowdhary, T. Harmel, and F. Waquet, *Opt. Express*, vol. 23, no. 21, p. 27829, 2015.
- [10] Santer and Schmechtig, *App. Optics*, vol. 39, no. 3, 2000.
- [11] A. Huck, M. Guillaume, and J. Blanc-Talon, *IEEE TGRS*, vol. 48, no. 6, pp. 2590–2600, 2010.